EEET ECOLOGICAL ENGINEERING & ENVIRONMENTAL TECHNOLOGY

Ecological Engineering & Environmental Technology 2023, 24(5), 275–281
https://doi.org/10.12912/27197050/166010
ISSN 2719–7050, License CC-BY 4.0

Received: 2023.04.18
Accepted: 2023.05.20
Published: 2023.06.05

Adsorption of Phenol Using Hydrochar Modified Layered Double Hydroxide – Kinetic, Isotherm, and Regeneration Studies

Neza Rahayu Palapa[1], Nur Ahmad[2,3], Hasja Paluta Utami[3], Zaqiya Artha Zahara[3], Risfidian Mohadi[2], Aldes Lesbani[2,3*]

[1] Department of Chemistry, Faculty of Mathematics and Natural Sciences, Universitas Sriwijaya, Indonesia
[2] Graduate School of Mathematics and Natural Sciences, Faculty of Mathematics and Natural Sciences, Universitas Sriwijaya, Indonesia
[3] Research Center of Inorganic Materials and Coordination Complexes, Faculty of Mathematics and Natural Sciences, Universitas Sriwijaya, Indonesia
* Corresponding author's e-mail: aldeslesbani@pps.unsri.ac.id

ABSTRACT

In this work, hydrochar using to modified nickel aluminum layered double hydroxide (hydrochar@NiAl LDH). The collected data by XRD indicate that 2θ of material at 11.38°, 22.90°, 35.20°, and 61.60°. The FTIR spectrum of hydrochar@NiAl LDH at wavenumber 3448, 1650, 1500–1600, 1348, 1056, and 500–800 cm^{-1}. NiAl LDH and hydrochar have surface areas of 3.288 m^2/g and 7.366 m^2/g, respectively. The precursors enhance the composite's surface area by 11.879 m^2/g. NiAl LDH, hydrochar, and hydrochar@NiAl LDH have optimal pH values of 3, 6, and 6 respectively. The adsorption process is determined by the kinetic model of pseudo-second order and the model of Freundlich isotherm. NiAl LDH, hydrochar, and hydrochar@NiAl LDH had respective maximum adsorption capacities of 25.445, 21.008, and 25.773 mg/g. The increase in regeneration cycles decreases the percentage of adsorbed.

Keywords: layered double hydroxide; adsorption study; materials composites; water treatment.

INTRODUCTION

Together with the growing population and technological advancements, water contamination has become one of the most serious issues and a concern for numerous parties. Phenol is one of the harmful chemicals in environment (Chaari et al., 2021). Various sectors, such as metal fabrication, rubber, pharmaceuticals, paints, timber manufacturing, chemical insecticides, pulp, and paper, may produce phenol pollution (Dehmani, Lgaz, et al., 2021; Wang et al., 2022; J. Zhang et al., 2022).

The existence of phenol in the environment, especially in water, could be detrimental to aquatic communities and the safety of people (da Silva et al., 2022). The US Environmental Protection Agency (USEPA) defines a permitted level of 1 μg/L for phenol in water (de Farias et al., 2022). Thus, the adsorption method is one of the necessary solutions for addressing environmental contamination (Khan et al., 2022). Compared to other techniques, adsorption has a number of advantages, including a very uncomplicated procedure, a relatively high level of effectiveness, and an efficient use of resources (Jain et al., 2022).

The adsorbent must have an excellent ability to adsorb for the adsorption procedure to be successful. Scientists have utilized numerous adsorbents, including biochar, kaolin, metal organic gramework, and layered double hydroxide, to solve problems with environmental contamination (Ahmad et al., 2023; Angerasa et al., 2021; Wijaya et al., 2021; B. L. Zhang et al., 2020).

Layered double hydroxides (LDHs) is an anionic form of clay and hydrotalcite capable of interlayer ion exchange. Its general formula is $[M^{2+}_{1-x}M^{3+}_{x}(OH)_2]^{x+}$ $[(A^{n-})_{x/n}\cdot yH_2O]^x$, where M represents metal cations (Bouteraa et al., 2020; Ruan et al., 2016). Due to their superior adsorption and singularity, layered double hydroxides have been widely investigated as adsorbents (Tran et al., 2019).

The advancement of LDH materials was conducted on a hydrochar-based structure. Juleanti et al. (2022) examined the direct green adsorption capacities of M^{2+}/Al (M = Ca, Mg, Zn) composites based on hydrochar. Moreover, LDH can be combined with hydrochar. Hydrochar is a recognized adsorbent, therefore it can be used to remove dangerous substances from certain wastes. According to Barbusinski et al. (2016), hydrochar is a well-known and effective biopolymer for remediation of water. Hydrochar possesses physical and chemical qualities, strong reactivity, and high pollution selectivity (Seedao et al., 2018).

In this work, the NiAl LDH composite will be modified using hydrochar. Brunauer Emmett Teller (BET), Fourier Transform Infra-Red (FTIR), X-Ray Diffraction (XRD) and were used to characterize the produced composite materials. Hydrochar@NiAl LDH will be used as an adsorbent for phenol-based organic molecules. The adsorption parameters as kinetics, isotherms, and regeneration must be assessed. Therefore, variations of pH, concentration, time of contact, temperature, and desorption process will be studied.

EXPERIMENTAL SECTION

Chemicals and instrumentation

Phenol (C_6H_5OH), distilled water (H_2O), 4-aminoantipyrine ($C_{11}H_{13}N_3O$), nickel hexahydrate ($Ni(NO_3)_2\cdot 6H_2O$), potassium hexacyanoferrate(III) ($K_3[Fe(CN)_6]$), aluminum nitrate nonahydrate ($Al(NO_3)_3\cdot 9H_2O$), acetate buffer solution (CH_3COONa) pH 10, sodium carbonate (Na_2CO_3), hydrochar, hydrogen chloride (HCl), and sodium hydroxide (NaOH) were used without any further purification. Instrumentation for characterization of adsorbents is Surface Area Analyzer (Brunauer Emmet Teller, (BET)), X-Ray Diffraction (XRD), UV-Vis spectrophotometer, and Fourier Transform Infra-Red (FTIR).

Preparation Hydrochar@NiAl LDH

30 mL of 0.75 M $Ni(NO_3)_2\cdot 6H_2O$ was combined with 30 mL of 0.25 M $Al(NO_3)_2\cdot 9H_2O$, agitated, and then 3 g of hydrochar was added. Slowly, the 2 M NaOH solution was added to the mixture until the pH reached 10; the final pH was 10. After three days of churning at 80°C, solids were created. The substance was subsequently filtered and rinsed with distilled water. The hydrochar@NiAl LDH was dried at 80°C.

Adsorption of phenol

Variations in pH, time of contact, concentration of phenol, temperature reaction, and the regeneration procedure were used to investigate adsorption parameters. An Erlenmeyer holding 20 mL of phenol was loaded with 0.02 g of adsorbent. Adsorption was conducted with varying pH (2–11), contact period (0–180 min), initial concentration of phenol (10–30 mg/L), temperature reaction (30–60°C), and regeneration cycle frequency (5 times). The phenol solution then became complexed.

According to Xie et al. (2020), 1 mL of a 5 mg/L phenol solution was added to a beaker to initiate the phenol complex procedure. Then 0.1 mL of a 2% $C_{11}H_{13}N_3O$, 0.1 mL of an 8% $K_3[Fe(CN)_6]$, buffer solution (pH 10) 1 mL, and distilled water 3 mL were added, respectively. The phenol complex was thereafter homogenized for 10 min. Finally, the concentration of phenol after adsorption was measured at 505.2 nm using a UV-Visible spectrophotometer.

RESULTS AND DISCUSSION

XRD diffractogram were used to construct a hydrochar@NiAl LDH for characterization, as shown in Fig. 1. The collected data indicate that 2θ at 11.38°(003), 22.90°(006), 35.20°(012), and 61.60°(110). The JCPDS No.15–0015 demonstrates the success of the NiAl LDH synthesis (Ahmad et al., 2022). Characterization XRD of Hydrochar@NiAl LDH revealed that the characteristic peaks of LDH were observed at 2θ = 11.38°, 35.20°, and 61.60°, even though the typical peaks of hydrochar were observed at 2θ = 22.90°.

The FTIR spectrum of the hydrochar@NiAl LDH composite material is depicted in Figure 2.

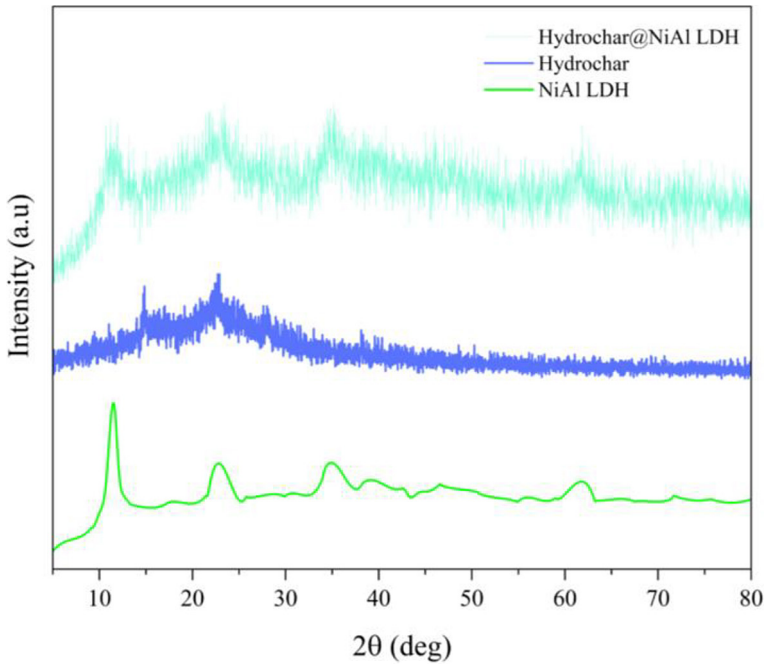

Fig. 1. X-Ray diffractogram of adsorbents

Water molecules exhibit vibrations with a wavenumber of 3448 cm^{-1} in their -OH group. In the NiAl composite, the O-H bending frequency is 1650 cm^{-1}. At 1500–1600 cm^{-1}, the C=C bonding from hydrochar is visible. The nitrate group in LDH has a wavenumber of 1348 cm^{-1}, the C-O vibration in hydrochar has a wavenumber of 1056 cm^{-1}, and the band for M-O is between 500 and 800 cm^{-1}.

The visual representations of the nitrogen adsorption-desorption isotherms of NiAl LDH, hydrochar, and hydrochar@NiAl LDH are shown in Figure 3. Based on the IUPAC categorization, every material corresponds to a type IV isotherm. If the material being used adsorbent has pores the size range of material is 2–50 nm and become filled with nitrogen (El Hassani et al., 2017). NiAl LDH and hydrochar have surface

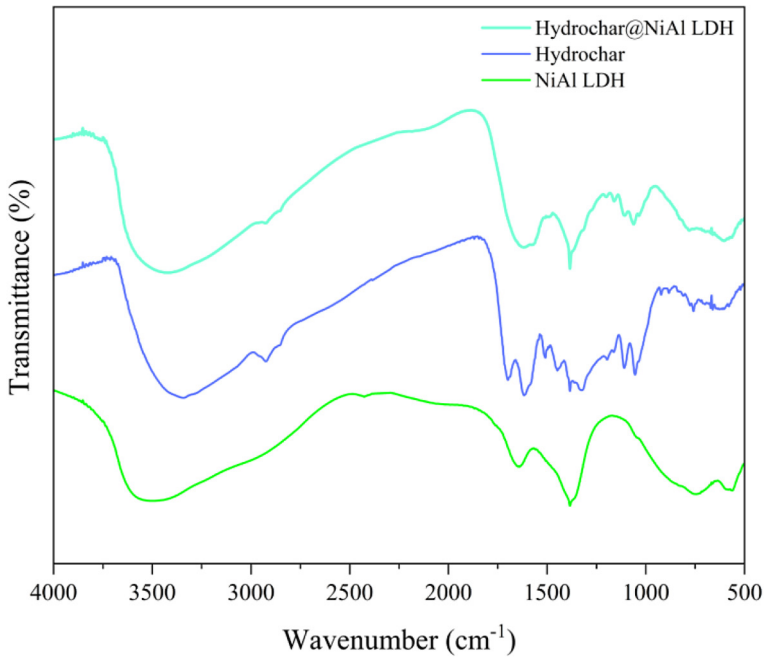

Fig. 2 Fourier transfer infra-red spectrum of adsorbents

Table 1. Brunauer Emmet Teller of adsorbents

Parameter	NiAl LDH	Hydrochar	Hydrochar@NiAl LDH
Surface area (m^2/g)	3.288	7.366	11.879
Pore volume (cm^3/g), BJH	0.006	0.008	0.013
Pore size (nm), BJH	16.983	3.189	2.205

areas of 3.288 m^2/g and 7.366 m^2/g, respectively. The building blocks enhance the composite's surface area by 11.879 m^2/g. Therefore, according to Table 1, it could have verified that the LDH improvement procedure with hydrochar was useful and led to a raised surface area.

The influence of pH is crucial to the treatment process (Ullah et al., 2022). Fig. 4 depicts the optimal pH of NiAl LDH to be 3, with an adsorp of 13.355 mg/L. The optimal pH for hydrochar and hydrochar@NiAl LDH material is 6, with an adsorbed hydrochar concentration of 12.744 mg/L and a concentration of 14.671 mg/L for hydrochar@NiAl LDH. Cited Al-Ghouti et al. (2022), graphite oxide is positively charged when the solution's pH is low or when the solution is acidic, whereas the adsorbent's surface is negatively charged in alkaline solutions.

The information impact of phenol by interaction time was utilized in Fig. 5. The reaction rate was determined using pseudo-first order (PFO) and pseudo-second order (PSO) kinetics model. The kinetic model is determined by observing how near the value of the coefficient of determination (R^2) becomes 1, the minimal value of the reaction rate (k), and the similarities between the measured and calculated Qe. According to Table 2, every adsorbent substance is compatible with the PSO. The close connection of the coefficient of determination (R^2) to 1 demonstrates this, and since the value of the reaction's kinetic rate (k_2) in the PSO is lower than PFO, the reaction proceeds more swiftly in the PSO. The phenol adsorption by PSO suggested chemisorption (Gao et al., 2022).

When adsorption reaction involves monolayer form and molecules of adsorbate interact, the Langmuir isotherm is utilized. The Freundlich isotherm theory applies to processes of adsorption involving in two or more layers without adsorbate molecule interaction and separation (Liu et al., 2021). The findings of adsorption isotherm calculations for NiAl LDH, hydrochar, and hydrochar@NiAl LDH are presented in Table 3. In lines with the Freundlich model, the correlation coefficient (R^2) was closer to 1 for all adsorbents. NiAl LDH, hydrochar, and hydrochar@NiAl LDH have respective maximal adsorption capacities of 25.445, 21.008, and 25.773 mg/g. This study's maximal adsorption capacities are compared to those of other studies in Table 4.

Figure 6 demonstrates that during the third regeneration, the adsorbent regeneration process

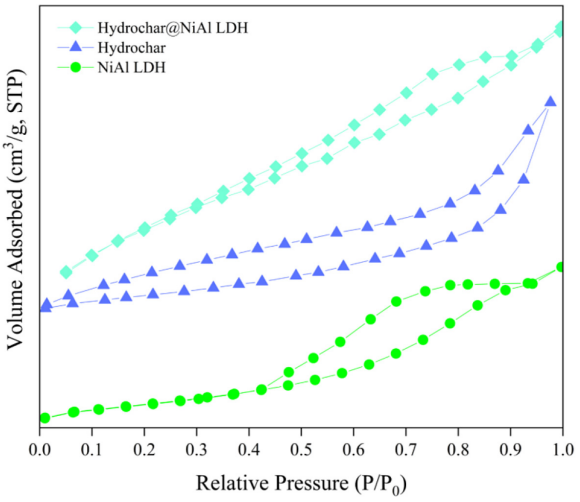

Fig. 3. N_2 adsorption-desorption isotherm of NiAl LDH, hydrochar, and hydrochar@NiAl LDH

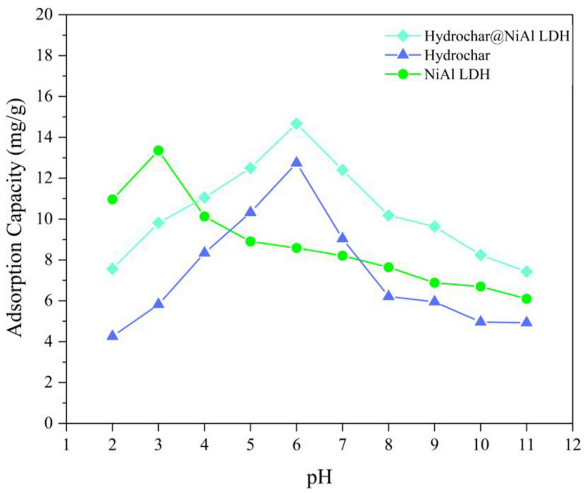

Fig. 4. Effect of pH

Table 2. PFO and PSO kinetic models

Adsorbents	Qe_{exp} (mg/g)	PFO			PSO		
		Qe_{calc} (mg/g)	k_1 (min^{-1})	R^2	Qe_{calc} (mg/g)	k_2 (g/mg.min)	R^2
NiAl LDH	12.274	7.224	0.030	0.9719	12.804	0.010	0.9997
Hydrochar	8.929	8.587	0.046	0.9315	9.379	0.011	0.9987
Hydrochar@NiAl LDH	14.821	9.598	0.027	0.9713	15.552	0.006	0.9976

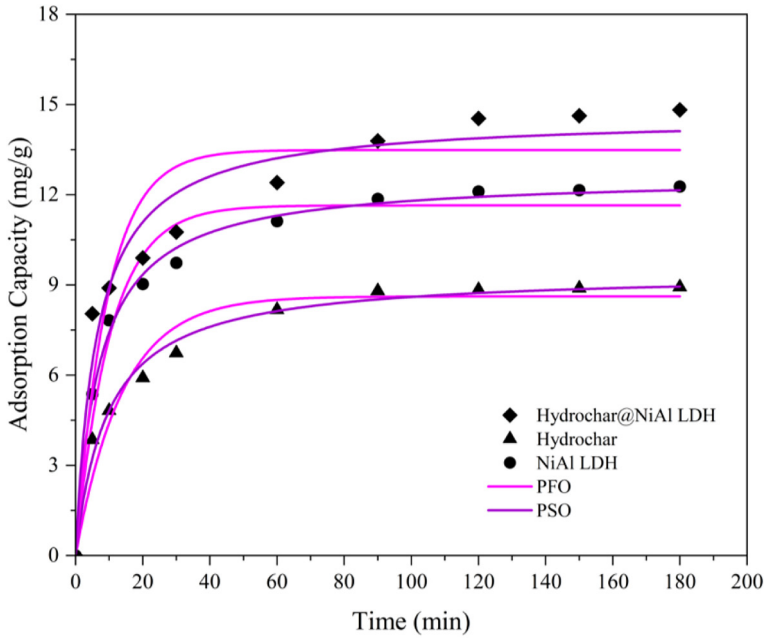

Fig. 5. PFO and PSO kinetic model

slowed down. The proportion of phenol absorbed by NiAl LDH, hydrochar, and hydrochar@NiAl LDH after a run regeneration was 47.821, 40.665, and 56.567%, respectively. The proportion of adsorbed decreases as the number of regeneration cycles increases; the percentage adsorbed of phenol after 5 run regeneration to 3.545%, 1.845%, and 12.200%, respectively.

Table 3. Isotherm parameter adsorption of phenol

Adsorbent	T (°C)	Langmuir			Freundlich		
		Q_{max}	kL	R^2	n	kF	R^2
NiAl LDH	30	25.445	0.438	0.845	1.395	1.456	0.9478
	40	25.063	0.055	0.8827	1.466	1.801	0.9447
	50	23.041	0.079	0.9392	1.653	2.469	0.9516
	60	24.155	0.088	0.9451	1.685	2.820	0.9548
Hydrochar	30	21.008	0.036	0.6816	1.345	1.009	0.8955
	40	19.531	0.047	0.8232	1.451	1.245	0.9173
	50	17.007	0.068	0.9185	1.648	1.655	0.9234
	60	17.606	0.072	0.9224	1.665	1.795	0.9230
Hydrochar@NiAl LDH	30	25.773	0.047	0.8467	1.412	1.583	0.9440
	40	22.936	0.069	0.9165	1.570	2.107	0.9432
	50	22.727	0.084	0.9441	1.664	2.545	0.9490
	60	24.213	0.096	0.9429	1.706	3.011	0.9516

Table 4. Assessment of maximum phenol adsorption capacity with previous study

Adsorbent	Q_{max} (mg/g)	Reference
α-Fe_2O_3	21.93	(Dehmani et al., 2020)
Zn_4Al-LDH	7.73	(Lupa et al., 2018)
Clarified sludge	1.052	(Mandal & Das, 2019)
Tea waste	7.62	(Gupta & Balomajumder, 2015)
Bentonite	23.64	(Ahmadi & Igwegbe, 2018)
Natural clay	10.1	(Dehmani, Khalki, et al., 2021)
Lignite	6.216	(Liu et al., 2021)
Hydrochar@NiAl LDH	25.773	This study

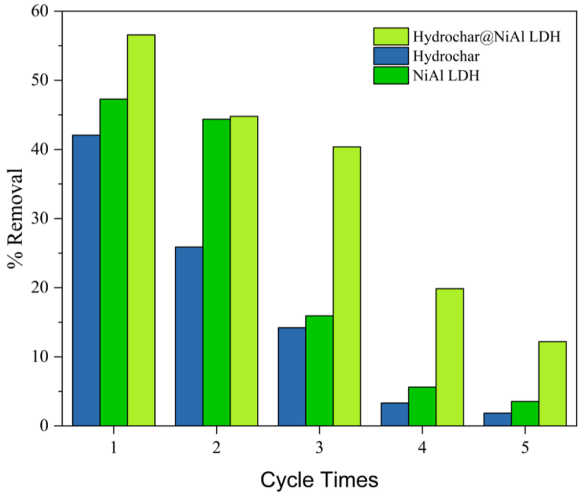

Fig. 6. Regeneration study of adsorbent

CONCLUSION

Characterization by XRD, FTIR, and BET revealed that the composite NiAl LDH with hydrochar was successful. NiAl LDH has an optimal pH of 3, whereas hydrochar and hydrochar@NiAl LDH materials have an optimal pH of 6. In the adsorption process, the kinetic and isotherm models are respectively pseudo-second-order and Freundlich. NiAl LDH, hydrochar, and hydrochar@NiAl LDH had respective maximum adsorption capacities of 25.445, 21.008, and 25.773 mg/g. The increase in regeneration cycles decreases the percentage of adsorbed.

Acknowledgements

The authors thank the Research Centre of Inorganic Materials and Coordination Complexes FMIPA Universitas Sriwijaya for support and instrumental analysis.

REFERENCES

1. Ahmad, N., Wijaya, A., Salasia Fitri, E., Suryani Arsyad, F., Mohadi, R., Lesbani, A. 2022. Catalytic Oxidative Desulfurization of Dibenzothiophene by Composites Based Ni/Al-Oxide. In Science and Technology Indonesia, 7(3). https://doi.org/11.26554/sti.2222.7.3.385–391
2. Ahmadi, S., Igwegbe, C.A. 2018. Adsorptive removal of phenol and aniline by modified bentonite: adsorption isotherm and kinetics study. Applied Water Science, 8(6). https://doi.org/10.1007/s13201–018–0826–3
3. Al-Ghouti, M.A., Sayma, J., Munira, N., Mohamed, D., Da'na, D.A., Qiblawey, H., Alkhouzaam, A. 2022. Effective removal of phenol from wastewater using a hybrid process of graphene oxide adsorption and UV-irradiation. Environmental Technology and Innovation, 27. https://doi.org/10.1016/j.eti.2022.102525
4. Alves, D.C.S., Gonçalves, J.O., Coseglio, B.B., Burgo, T.A.L., Dotto, G.L., Pinto, L.A.A., Cadaval, T.R.S. 2019. Adsorption of phenol onto chitosan hydrogel scaffold modified with carbon nanotubes. Journal of Environmental Chemical Engineering, 7(6). https://doi.org/10.1016/j.jece.2019.103460
5. Asnaoui, H., Dehmani, Y., Khalis, M., Hachem, E.K. 2020. Adsorption of phenol from aqueous solutions by Na–bentonite: kinetic, equilibrium and thermodynamic studies. International Journal of Environmental Analytical Chemistry. https://doi.org/10.1080/03067319.2020.1763328
6. Barbusinski, K., Salwiczek, S., Paszewska, A. 2016. The Use of Chitosan For Removing Selected Pollutants From Water And Wastewater – Short Review. Architecture, Civil Engineering, Environment, 9, 107–115. https://doi.org/10.21307/acee-2016–026
7. Bouteraa, S., Saiah, F.B.D., Hamouda, S., Bettahar, N. 2020. Zn-M-CO3 layered double hydroxides (M=Fe, Cr, or Al): Synthesis, characterization, and removal of aqueous indigo carmine. Bulletin of Chemical Reaction Engineering & Catalysis, 15(1), 43–54. https://doi.org/10.9767/bcrec.15.1.5053.43–54
8. Cao, Y., Wang, Y., Zhou, F., Huang, J., Xu, M. 2022. Acylamino-functionalized hyper-cross-linked polymers for efficient adsorption removal of phenol in aqueous solution. Separation and Purification Technology, 303, 122229. https://doi.org/10.1016/j.seppur.2022.122229
9. da Silva, M.C.F., Schnorr, C., Lütke, S.F., Knani, S., Nascimento, V.X., Lima, É.C., Thue, P.S., Vieillard, J., Silva, L.F.O., Dotto, G.L. 2022. KOH activated carbons from Brazil nut shell: Preparation, characterization, and their application in phenol adsorption. Chemical Engineering Research and Design, 187, 387–396. https://doi.org/10.1016/j.cherd.2022.09.012
10. de Farias, M.B., Prediger, P., Vieira, M.G.A. 2022. Conventional and green-synthesized nanomaterials applied for the adsorption and/or degradation of phenol: A recent overview. In Journal of

Cleaner Production. Elsevier Ltd, 367. https://doi.org/10.1016/j.jclepro.2022.132980

11. de La Luz-Asunción, M., Sánchez-Mendieta, V., Martínez-Hernández, A.L., Castaño, V.M., Velasco-Santos, C. 2015. Adsorption of phenol from aqueous solutions by carbon nanomaterials of one and two dimensions: Kinetic and equilibrium studies. Journal of Nanomaterials, 2015. https://doi.org/10.1155/2015/405036
12. Dehmani, Y., Alrashdi, A.A., Lgaz, H., Lamhasni, T., Abouarnadasse, S., Chung, I.M. 2020. Removal of phenol from aqueous solution by adsorption onto hematite (α-Fe2O3): Mechanism exploration from both experimental and theoretical studies. Arabian Journal of Chemistry, 13(5), 5474–5486. https://doi.org/10.1016/j.arabjc.2020.03.026
13. Dehmani, Y., Khalki, O., El, Mezougane, H., Abouarnadasse, S. 2021. Comparative study on adsorption of cationic dyes and phenol by natural clays. Chemical Data Collections, 33. https://doi.org/10.1016/j.cdc.2021.100674
14. Dehmani, Y., Lgaz, H., Alrashdi, A.A., Lamhasni, T., Abouarnadasse, S., Chung, I.M. 2021. Phenol adsorption mechanism on the zinc oxide surface: Experimental, cluster DFT calculations, and molecular dynamics simulations. Journal of Molecular Liquids, 324. https://doi.org/10.1016/j.molliq.2020.114993
15. Gao, W., Lin, Z., Chen, H., Yan, S., Zhu, H., Zhang, H., Sun, H., Zhang, S., Zhang, S., Wu, Y. 2022. Roles of graphitization degree and surface functional groups of N-doped activated biochar for phenol adsorption. Journal of Analytical and Applied Pyrolysis, 167, 105700. https://doi.org/10.1016/j.jaap.2022.105700
16. Gupta, A., Balomajumder, C. 2015. Simultaneous removal of Cr(VI) and phenol from binary solution using Bacillus sp. immobilized onto tea waste biomass. Journal of Water Process Engineering, 6, 1–10. https://doi.org/10.1016/j.jwpe.2015.02.004
17. Jain, M., Khan, S.A., Sahoo, A., Dubey, P., Pant, K.K., Ziora, Z.M., Blaskovich, M.A.T. 2022. Statistical evaluation of cow-dung derived activated biochar for phenol adsorption: Adsorption isotherms, kinetics, and thermodynamic studies. Bioresource Technology, 352. https://doi.org/10.1016/j.biortech.2022.127030
18. Juleanti, N., Normah, N., Siregar, P.M.S.B.N., Wijaya, A., Palapa, N.R., Taher, T., Hidayati, N., Mohadi, R., Lesbani, A. 2022. Comparison of the Adsorption Ability of MgAl-HC, CaAl-HC, and ZaAl-HC Composite Materials Based on Duku Peel Hydrochar in Adsorption of Direct Green Anionic Dyes. Indonesian Journal of Chemistry, 22(1), 192–204. https://doi.org/10.22146/ijc.68719
19. Khan, D., Kuntail, J., Sinha, I. 2022. Mechanism of phenol and p-nitrophenol adsorption on kaolinite surface in aqueous medium: A molecular dynamics study. Journal of Molecular Graphics and Modelling, 116. https://doi.org/10.1016/j.jmgm.2022.108251
20. Lesbani, A., Palapa, N.R., Sayeri, R.J., Taher, T., Hidayati, N. 2021. High reusability of NiAl LDH/biochar composite in the removal methylene blue from aqueous solution. Indonesian Journal of Chemistry, 21(2), 421–434. https://doi.org/10.22146/ijc.56955
21. Liu, X., Tu, Y., Liu, S., Liu, K., Zhang, L., Li, G., Xu, Z. 2021. Adsorption of ammonia nitrogen and phenol onto the lignite surface: An experimental and molecular dynamics simulation study. Journal of Hazardous Materials, 416. https://doi.org/10.1016/j.jhazmat.2021.125966
22. Lupa, L., Cocheci, L., Pode, R., Hulka, I. 2018. Phenol adsorption using Aliquat 336 functionalized Zn-Al layered double hydroxide. Separation and Purification Technology, 196, 82–95. https://doi.org/10.1016/j.seppur.2017.10.003
23. Mandal, A., Das, S.K. 2019. Phenol adsorption from wastewater using clarified sludge from basic oxygen furnace. Journal of Environmental Chemical Engineering, 7(4). https://doi.org/10.1016/j.jece.2019.103259
24. Qu, Y., Qin, L., Liu, X., Yang, Y. 2022. Magnetic Fe3O4/ZIF-8 composite as an effective and recyclable adsorbent for phenol adsorption from wastewater. Separation and Purification Technology, 294. https://doi.org/10.1016/j.seppur.2022.121169
25. Ruan, X., Chen, Y., Chen, H., Qian, G., Frost, R.L. 2016. Sorption behavior of methyl orange from aqueous solution on organic matter and reduced graphene oxides modified Ni-Cr layered double hydroxides. Chemical Engineering Journal, 297, 295–303. https://doi.org/10.1016/j.cej.2016.01.041
26. Sathya Priya, D., Sureshkumar, M.V. 2020. Synthesis of Borassus flabellifer fruit husk activated carbon filter for phenol removal from wastewater. International Journal of Environmental Science and Technology, 17(2), 829–842. https://doi.org/10.1007/s13762–019–02325–3
27. Seedao, C., Rachphirom, T., Phiromchoei, M., Jangiam, W. (n.d.). Anionic Dye Adsorption from Aqueous Solutions by Chitosan Coated Luffa Fibers.
28. Taher, T., Putra, R., Rahayu Palapa, N., Lesbani, A. 2021. Preparation of magnetite-nanoparticle-decorated NiFe layered double hydroxide and its adsorption performance for congo red dye removal. Chemical Physics Letters, 777(February), 138712. https://doi.org/10.1016/j.cplett.2021.138712
29. Wang, P., Geng, X., Luo, L., Liu, Y., Eglitis, R.I., Wang, X. 2022. The adsorption behavior of phenol on the surface of 1D/2D M@MoS2 (M = Co and Rh) for hydrodeoxidation reaction: Insights from theoretical investigations. Applied Surface Science, 601. https://doi.org/10.1016/j.apsusc.2022.154242
30. Xie, B., Qin, J., Wang, S., Li, X., Sun, H., Chen, W. 2020. Adsorption of Phenol on Commercial Activated Carbons: Modelling and Interpretation. International Journal of Environmental Research and Public Health, 17(3). https://doi.org/10.3390/ijerph17030789
31. Zhang, J., Liu, N., Gong, H., Chen, Q., Liu, H. 2022. Hydroxyl-functionalized hypercrosslinked polymers with ultrafast adsorption rate as an efficient adsorbent for phenol removal. Microporous and Mesoporous Materials, 336. https://doi.org/10.1016/j.micromeso.2022.111836